# How Much Do Tropical Cyclones Affect Seasonal and Interannual Rainfall Variability over the Western North Pacific?

HISAYUKI KUBOTA

*Research Institute for Global Change, Japan Agency for Marine-Earth Science and Technology, Yokosuka-city, Japan*

BIN WANG*

*Department of Meteorology, and International Pacific Research Center, University of Hawaii at Manoa, Honolulu, Hawaii*

(Manuscript received and in final form 28 April 2009)

ABSTRACT

The authors investigate the effects of tropical cyclones (TCs) on seasonal and interannual rainfall variability over the western North Pacific (WNP) by using rainfall data at 22 stations. The TC-induced rainfall at each station is estimated by using station data when a TC is located within the influential radius (1000 km) from the station. The spatial–temporal variability of the proportion of TC rainfall is examined primarily along the east–west island chain near 10°N (between 7° and 13°N) and the north–south island chain near 125°E (between 120° and 130°E).

Along 10°N the seasonality of total rainfall is mainly determined by non-TC rainfall that is influenced by the WNP monsoon trough. The proportion of the TC rain is relatively low. During the high TC season from July to December, TC rainfall accounts for 30% of the total rainfall in Guam, 15%–23% in Koror and Yap, and less than 10% at other stations. In contrast, along 125°E where the WNP subtropical high is located, the TC rainfall accounts for 50%–60% of the total rainfall between 18° and 26°N during the peak TC season from July to October. In Hualien of Taiwan, TC rainfall exceeds 60% of the total rainfall.

The interannual variability of the TC rainfall and total rainfall is primarily modulated by El Niño–Southern Oscillation (ENSO). Along 10°N, the ratio of TC rainfall versus total rainfall is higher than the climatology during developing and mature phases of El Niño (from March to the following January), whereas the ratio is below the climatology during the decaying phase of El Niño. The opposite is true for La Niña, except that the impact of La Niña is shorter in duration. Furthermore, in summer of El Niño developing years, the total seasonal rainfall increases primarily because of the increase of TC rainfall. In the ensuing autumn, an anticyclonic anomaly develops over the Philippine Sea and TC rainfall shifts eastward; as a result, the total rainfall over the Philippines and Taiwan decreases. The total rainfall to the east of 140°E, however, changes little, because the westward passage of TCs enhances TC rainfall, which offsets the decrease of non-TC rainfall. Along the meridional island chain between 120° and 130°E, the total rainfall anomaly is affected by ENSO starting from the autumn to the following spring, and the variation in TC rainfall dominates the total rainfall variation only in autumn (August–November) of ENSO years.

The results from this study suggest that in the tropical WNP and subtropical East Asian monsoon regions (east of 120°E), the seasonal and interannual variations of rainfall are controlled by changes in nonlocal circulations. These changes outside the monsoon domain may substantially affect summer monsoon rainfall by changing TC genesis and tracks.

## 1. Introduction

A tropical cyclone (TC) produces heavy rainfall and strong winds along its passage, having a great effect on the environment. Over the western North Pacific (WNP), TC formation is affected by the phase of El Niño–Southern Oscillation (ENSO; Atkinson 1977; Chan 1985, 2000; Dong 1988; Wu and Lau 1992; Lander

* Visiting Professor at the Ocean University of China, Qingdao, China.

*Corresponding author address:* Hisayuki Kubota, RIGC, JAMSTEC, 2-15 Natsushima-cho, Yokosuka-city, Kanagawa, 237-0061, Japan.
E-mail: kubota@jamstec.go.jp

DOI: 10.1175/2009JCLI2646.1

1993, 1994; Chen et al. 1998; Wang and Chan 2002). It has also been reported that TCs tend to form more toward the east during El Niño. Chen et al. (1998) showed that the frequency of TC formation during the summer from June through August (JJA) in El Niño (La Niña) years increased (decreased) in the southern part of the WNP. However, the annual number of TCs in the WNP is not significantly correlated with ENSO (Lander 1993, 1994). Wang and Chan (2002) found that TC tracks tend to curve northward and TC life spans become longer during El Niño. Camargo and Sobel (2005) pointed out that TCs become more intense during El Niño.

The number of TC landfalls in Southeast Asia usually increases during the summer and autumn monsoon seasons. During the summer of an El Niño developing year, the number of TC making landfall increases in this area; however, the number decreases in the autumn (Wu et al. 2004; Fudeyasu et al. 2006; Lyon and Camargo 2008). When the TC genesis region shifts eastward from the autumn of an El Niño developing year, the TC rainfall distribution is relocated. How much influence does TC rainfall have on the regional rainfall climatology? Since each TC has a lot of variation, it is difficult to evaluate a TC's effect on climatological rainfall.

Rodgers et al. (2000) first estimated monthly TC rainfall using Special Sensor Microwave Imager (SSM/I) satellite data. They indicated that about 12% of the climatological rainfall over the WNP from June to November is due to TCs. They also found that TC rainfall is enhanced from 12%–18% of the total rainfall during El Niño. On the other hand, the total rainfall in the WNP tends to decrease from autumn to spring during El Niño (Ropelewski and Halpert 1987). Rodgers et al. (2000) did not quantify how much influence the increase of TC rainfall contributes to the change in the total rainfall. The satellite data are not of sufficiently duration to evaluate the interannual variability of rainfall. In the case of the Philippines, Lyon et al. (2006) showed a contrast of seasonal rainfall variability in summer and autumn during ENSO. Lyon and Camargo (2008) examined this contrast by defining a box region around the Philippines using the Climate Prediction Center Merged Analysis of Precipitation (CMAP; Xie and Arkin 1996) rainfall data from 1979 to 2004. They concluded that the contrast was influenced by the contribution of TCs to the rainfall that increases 29.8% in summer but decreases 27.9% in autumn of El Niño developing years from the mean contribution. In this study, we will use the long-term rain gauge station data to evaluate the contribution of TC rainfall to the seasonal and interannual variability of the total rainfall over the WNP.

The data and the definition of TC rainfall are described in section 2. Climatological seasonality of TC rainfall is presented in section 3. Interannual variability of TC rainfall associated with ENSO is revealed in section 4. A summary of the results are given in section 5.

## 2. Data

### *a. Datasets*

Long-term daily station rainfall data at 22 stations in the WNP islands, the Philippines, Taiwan, and the southwest islands of Japan are used in this study (Fig. 1). The TCs over the WNP primarily move westward and/or northward. Therefore, stations on the east coast/side or small islands are chosen in the Philippines and Taiwan to investigate the effect of TCs. Rainfall data from eight stations over the western Pacific islands (Koror, Yap, Guam, Ponape, Kwajalein, Majuro, and Wake Island) from 1951 to 2005 were downloaded from the Pacific Rainfall database Web site (available online at http://pacrain.evac.ou.edu/). These data were collected by surface weather stations over the western Pacific region, deployed by the National Oceanic and Atmospheric Administration, and archived by the National Climatic Data Center. Seven stations (Davao, Cagayan, Catbalogan, ViracSynop, Baler, Aparri, and Basco) have data from 1961 to 2005, which were provided by the Philippine Atmospheric, Geophysical and Astronomical Services Administration. Two stations in Taiwan (Lanyu and Hualien) were used for the period from 1951 to 2005, which were provided by the Central Weather Bureau of Taiwan. Rainfall data at six stations in Japan (Miyakojima, Naha, Naze, Tanegashima, Chichijima, and Minami-torishima) from 1961 to 2005 were observed by the Japan Meteorological Agency and were provided by the Japan Meteorological Business Support Center.

The best track data from 1951 to 2005 are downloaded from the Joint Typhoon Warning Center (JTWC) Web site (available online at https://metocph.nmci.navy.mil/jtwc.php). TCs are defined from the stage of tropical depression and tracked until they are downgraded again to the tropical depression stage. However, extratropical cyclones are excluded. The dataset includes locations of TCs, center pressure, maximum wind speed, and classification of the intensity. The Hadley Center Global Sea Ice Sea Surface Temperature monthly dataset of $1° \times 1°$ spatial resolution (Rayner et al. 2003) is used to calculate sea surface temperature (SST) for the ENSO Niño-3.4 index. The classification of El Niño and La Niña years[1] follows Trenberth (1997).

[1] The El Niño developing years used in this study are 1951, 1953, 1957, 1963, 1965, 1968, 1969, 1972, 1976, 1977, 1979, 1982, 1986, 1987, 1991, 1993, 1994, 1997, 2002, and 2004, for a total of 20 yr. The La Niña developing years are 1954, 1955, 1956, 1964, 1970, 1971, 1973, 1974, 1975, 1984, 1988, 1995, 1998, 1999, and 2000, for a total of 15 yr.

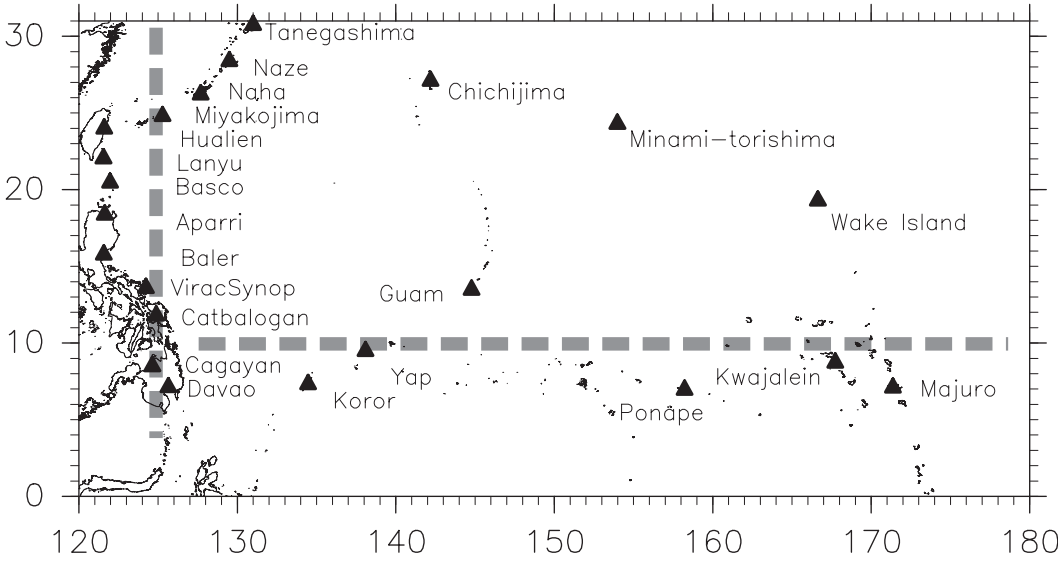


FIG. 1. Rain gauge stations used in this study. The two thick dashed lines along 10°N and 125°E mark locations of the east–west and north–south island chains, respectively.

### *b. Method for estimating TC-induced rainfall*

Frank (1977) derived an averaged TC rainfall distribution based on statistical analyses of 21-yr station data. He estimated that the mean rainfall within 4° of radius from the TC center was about 53.0 mm day$^{-1}$. Rodgers and Adler (1981) and Rao and MacArthur (1994) estimated TC rainfall statistically by using microwave radiometer satellite measurements. Their estimated mean rain rates were 45.6 and 48.7 mm day$^{-1}$, respectively, within 444 km of radius from the TC center. These studies provided us with an averaged TC rainfall distribution in the core region of TC.

To estimate the TC-induced rainfall, we assume that the TC rain rate depends only on the distance from the TC center. The distance from the TC center to each station can be obtained from 6-hourly best-track data. Rainfall data can also be made available for every six hours by dividing quarterly the daily station data. Rainfall is then binned into 100-km intervals. TC rainfall averaged over 22 stations within 4° radius is 35.6 mm day$^{-1}$. An approximate 50-yr average of our TC rainfall is relatively smaller than that given by previous studies.

Figure 2 shows the daily rainfall as a function of the distance between the TC center and stations. This mean distribution is obtained by averaging profiles at the 22 stations. Bars indicate one standard deviation of individual stations from the mean. The rainfall has a maximum of 78 mm day$^{-1}$ in the most innermost circle with a radius of 100 km. The rainfall rate decreases with distance away from the TC center. When the distance is greater than 1000 km, the rainfall becomes nearly independent of the distance. This means that the influence of TCs is limited to a 1000-km radius on average. On the basis of this empirical relationship and TC tracks, we classify the TC-induced rainfall at each station only when a TC is within 1000-km distance from the station. The TC-induced rainfall at each station is an accumulation of the station rainfall during the TC passage. Monthly accumulated TC rainfall can be determined by the sum of individual TC rainfall. The residual (the total minus TC rainfall) is referred to as non-TC rainfall. (The limitations of the TC-induced rainfall calculation are explained in the appendix).

## 3. Seasonality of TC-induced rainfall

### *a. TC rainfall and non-TC rainfall*

Across the WNP, seven island stations were chosen to represent an east–west cross section along 10°N (roughly between 7° and 13°N; Fig. 1). Across the western edge of the WNP, the Philippine islands, Taiwan, and the southwest islands of Japan (from Miyakojima to Tanegashima) provide a meridional cross section along 125°E (roughly between 120° and 130°E).

Monthly distributions of the total rainfall, TC rainfall, and non-TC rainfall over selected stations along the two cross sections are presented in Fig. 3. Along 10°N, the maximum total rainfall appears in July in Koror and progressively later eastward, with the latest maximum rainfall occurring in October in Majuro (except for Ponape). The results here agree with the study by Wang (1994), who found the maximum month of convective

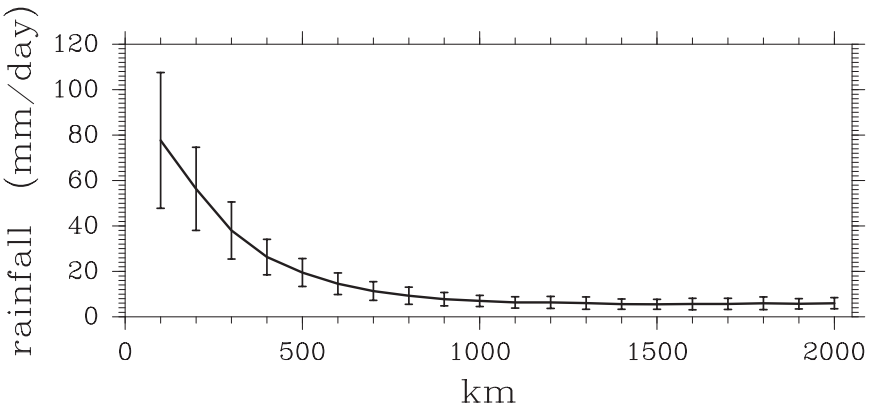


FIG. 2. Mean radial distribution of the TC rainfall from the TC center to a 2000-km radius. This mean distribution is derived by using 6-hourly TC track data and the rainfall data at 22 stations shown in Fig. 1. Bars indicate one standard deviation of the individual stations from their mean.

activity later in eastward region over the western and central North Pacific. The TC rainfall is larger in the western part of the WNP; however, its magnitude is smaller compared to the non-TC rainfall.

Along the north–south cross section of 125°E, non-TC rainfall increases clearly in May and June and decreases in July to the north of Baler. This non-TC rainfall is associated with the East Asian summer monsoon rainband during the Baiu/mei-yu season (Lau et al. 1988; Ninomiya and Akiyama 1992). The non-TC rainfall decreases when the rainband moves northward and the islands are under the influence of the WNP subtropical high. The TC rainfall, on the other hand, increases after July and reaches its peak in autumn. The TC rainfall maximum appears in August in Naze and progressively later southward: The peak appears in November in Catbalogan. The total rainfall shows double peaks in its annual variation: The first peak in May or June is due to non-TC rainfall and the second peak from August to October is primarily due to the TC rainfall. The TC rainfall is an important contributor to the total rainfall, especially in the regions where the WNP subtropical high prevails. Along the east coast of the Philippines, the northeasterly monsoon intensifies from September to January (Matsumoto 1992). The TC rainfall makes a considerable contribution to the total rainfall in the first half of the winter monsoon season. During the second half of the winter monsoon, non-TC rainfall becomes a dominant factor. In the southernmost part of the Philippines, Davao, TCs have little influence, and the seasonal variation of rainfall there is small.

### *b. Longitudinal and latitudinal distribution of TC rain ratio*

We define the TC rain ratio as monthly TC rainfall divided by monthly total rainfall. The monthly TC frequency, the monthly variation of the TC rain ratio, and the monthly average of the TC distance along 10°N are illustrated in Figs. 4a–4c. TC frequency is the number of TCs that approach the station and fall within the 1000-km radius from the station. The TC distance is the nearest distance of the TC to the station when it approaches the station and falls within the 1000-km radius from the station. High TC frequency appears west of Guam (from 125° to 150°E). TC frequency maximum appears from August to October in Guam, during October in Yap, and during November in Koror and Davao. The maximum TC rain ratio appears in October and November, which exceeds 35% in Guam. This maximum appears while the TC frequency is high. However, another maximum of the TC rain ratio appears in April and May from Koror to Ponape, which is not correlated with TC frequency. The TC distance tends to be closer (less than 500 km) when the TC rain ratio is high. High TC rain ratio from Koror to Ponape in April to May is associated with a smaller TC distance. Although the TC frequency is low, when a TC passes closer to the station, the TC produces more rainfall and increases the TC rain ratio. During March at Yap and in February at Ponape, in spite of very low TC frequency, TC distance from the station is less than 300 km. This means that once the TC approaches during these months, it passes very close to the station, and the risk of destructive damage is very high. On the contrary, the TC rain ratio is mostly less than 10% along this latitude to the eastmost island of Majuro and in the Philippines. During the high TC season from July to December, the maximum TC rain ratio reaches 30.2% on average in Guam. The ratio decreases to 14.7% and 22.8% in Koror and Yap, respectively, and to less than 10% at other stations (Table 1). At Davao, the TC frequency exceeds

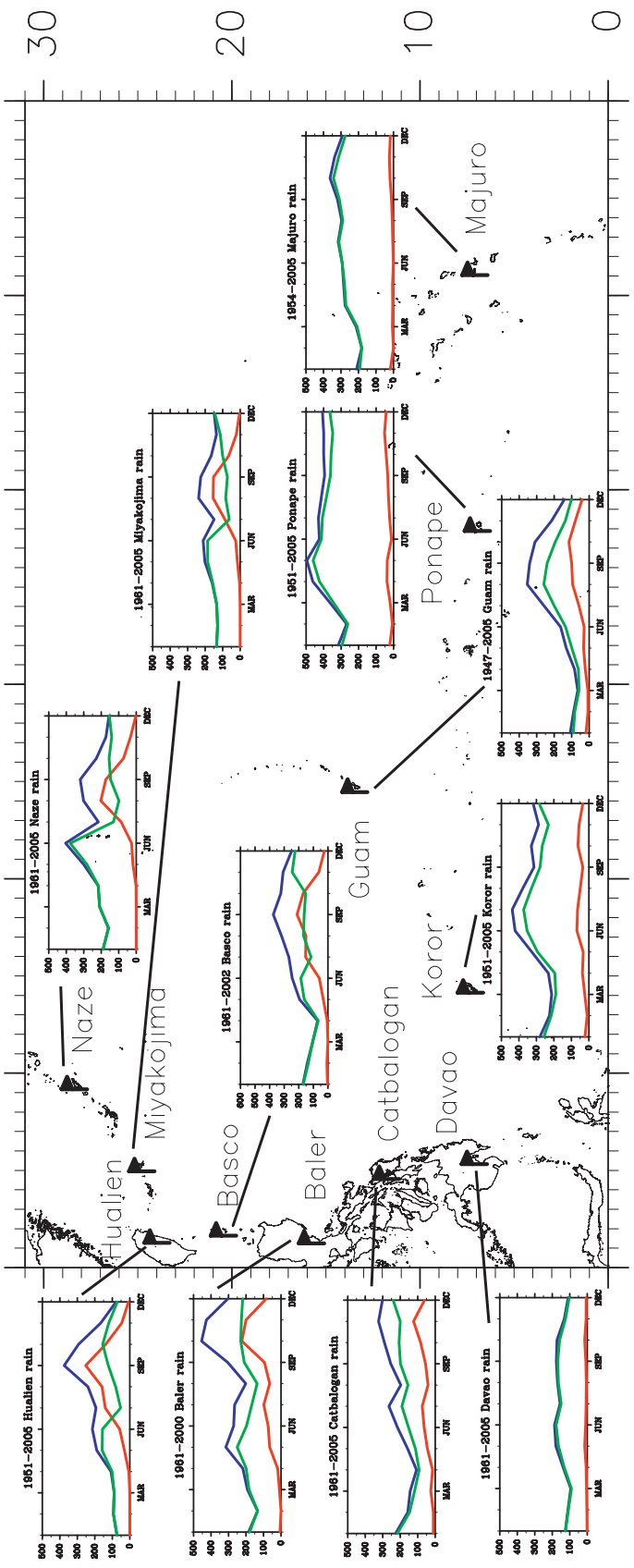


FIG. 3. Climatological seasonal distribution of the monthly total rainfall (blue), TC rainfall (red), and non-TC rainfall (green) at selected stations (units are mm). Abscissas indicate January through December.

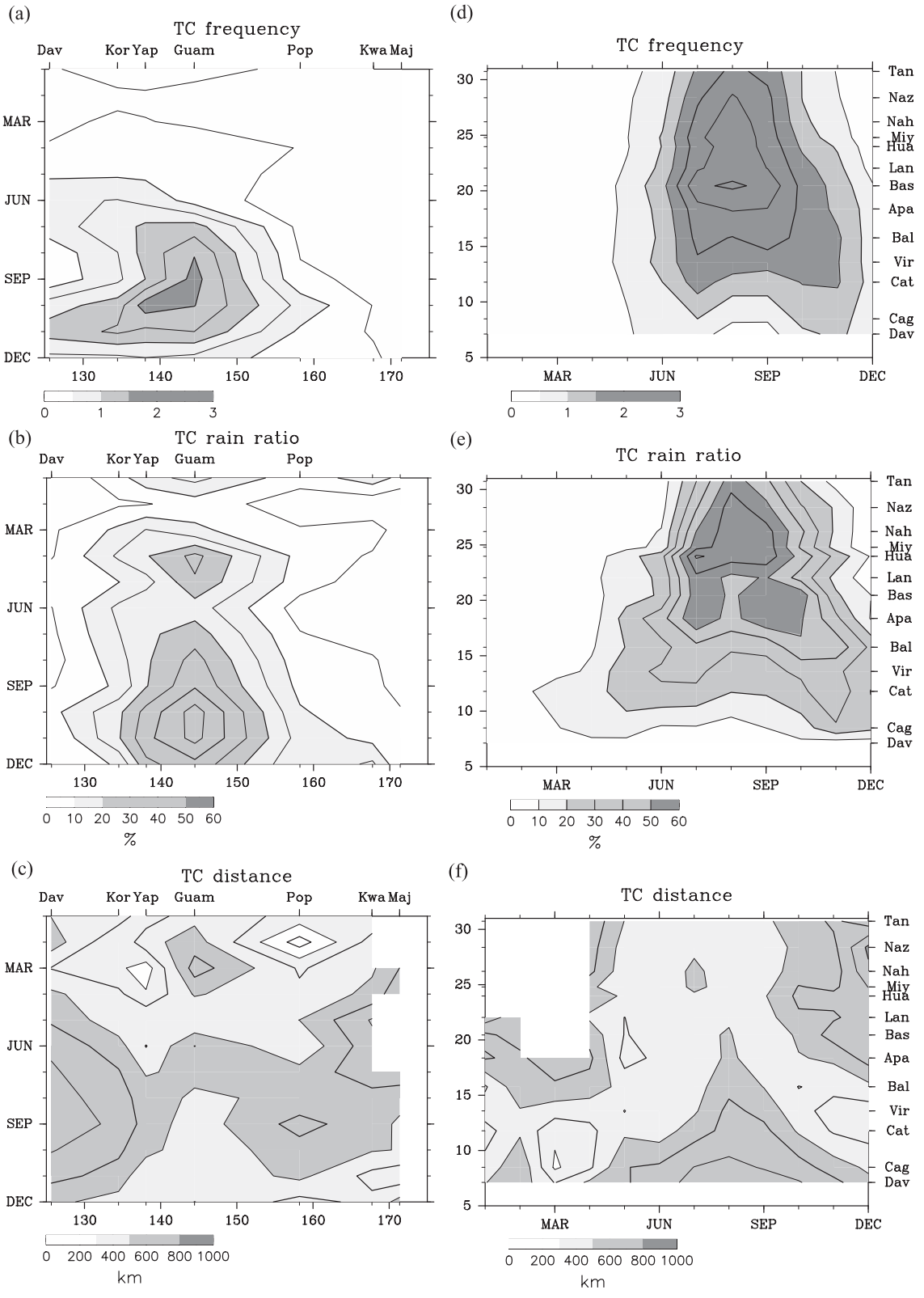


FIG. 4. Climatological-mean (a),(d) TC frequency, (b),(e) TC rain ratio, and (c),(f) TC distance along the east–west island chain between 7° and 13°N and the north–south island chain between 120° and 130°E, respectively, as shown in Fig. 1. The names of the stations are described in the abscissa in (a)–(c) and the ordinate in (d)–(f). Contour intervals are (a) 0.25 TC month$^{-1}$, (d) 0.5 TC month$^{-1}$, (b) 5%, (e) 10%, and (c),(f) 100 km.

TABLE 1. TC rain ratio averaged from July to December along the east–west island chain shown in Fig. 1.

| | TC rain ratio (%) |
|---|---|
| Koror | 14.7 |
| Yap | 22.8 |
| Guam | 30.2 |
| Ponape | 9.1 |
| Kwajalein | 7.5 |
| Majuro | 4.2 |

TABLE 2. As in Table 1, but averaged from July to October along the north–south island chain.

| | TC rain ratio (%) |
|---|---|
| Tanegashima | 37.0 |
| Naze | 47.2 |
| Naha | 55.7 |
| Miyakojima | 56.4 |
| Hualien | 62.2 |
| Lanyu | 47.8 |
| Basco | 53.4 |
| Aparri | 53.8 |
| Baler | 37.4 |
| Virac Synop | 28.5 |
| Catbalogan | 24.3 |
| Cagayan | 9.9 |
| Davao | 4.9 |

more than one per month in November, but its TC rain ratio is small because of the large TC distance.

The monthly TC frequency, TC rain ratio, and TC distance along the north–south cross section of 125°E are shown in Figs. 4d–4f. The northward (southward) migration of high TC frequency appears in July and August [from September to November (SON)]. The high TC rain ratio region corresponds to the high TC frequency region and period. The TC distance tends to be smaller (less than 500 km) when the TC rain ratio is high. From July to October, the TC rain ratio exceeds 50% north of Aparri (18°N) up to Tanegashima (30°N) and reaches 50%–60% on average between Aparri (18°N) and Naha (26°N) except for Lanyu (Table 2). The maximum ratio reaches 71% in July in Hualien, and its TC rain ratio exceeds 60% on average during the high TC season. However, the increase of the TC rain ratio before May is not associated with the increase of TC frequency. Even though the TC frequency is low, because the TCs approach is closer at south of Catbalogan (11°N) in March and April, the TC rain ratio increases.

## 4. Interannual variability of the TC rainfall

### *a. Composite TC rain ratio during El Niño and La Niña*

The interannual variability of the TC formation is strongly affected by ENSO phases (cf. Wang and Chan 2002). Thus, the seasonal TC rain ratio differs during El Niño and La Niña years. Since the mature stages of El Niño and La Niña usually occur in December, Fig. 5 includes both El Niño (La Niña) developing years and decaying years.

Figures 5a and 5c represent the anomalous three-month running mean of the TC frequency and the TC rain ratio along 10°N associated with El Niño. The significant eastward extension in the autumn of the El Niño developing year appeared in the TC frequency that corresponds to the eastward shift of TC genesis location during El Niño years (cf. Wang and Chan 2002). The TC rain ratio becomes higher than its climatology (except west of 140°E after September). The significantly positive TC rain-ratio anomaly region appears in Koror and Ponape in March of the developing year, which shifts to Guam in May. The high TC rain-ratio region shifts toward Majuro from October to the following January, corresponding to the significant increase of the TC frequency. In El Niño decaying years, the TC rain ratio becomes lower than its climatology because of the decrease of TC frequency associated with the dominance of the anomalous Philippine Sea anticyclone, which severely suppresses the local TC activity. The Philippine Sea anticyclonic anomalies are established during the autumn of El Niño developing years (Wang and Zhang 2002) and expand eastward from winter (mature phase of El Niño) to the following summer. The maintenance of the Philippine Sea anticyclonic anomalies is mainly due to a positive feedback between the moist atmosphere Rossby waves and the underlying SST dipole anomalies in the off-equatorial region (Wang et al. 2000).

During La Niña developing years, the TC frequency and the TC rain ratio are lower than its climatology (except west of 140°E after September). The significantly negative anomaly pattern of the TC rain ratio and the TC frequency during La Niña developing years is opposite to that of positive anomalies during El Niño developing years (Figs. 5b and 5d). In the spring of La Niña decaying years, the TC rain ratio has a positive anomaly in Guam, though it is below the significant level.

Figure 6 shows the north–south cross section of the anomalous three-month running mean of the TC frequency and the TC rain ratio along 125°E in both El Niño (La Niña) developing and decaying years. During the summer of El Niño developing years, the TC frequency is higher than its climatology in all regions and becomes lower in September (Lyon and Camargo 2008). The decrease of TC frequency only reaches the significant level. A similar contrast of increase in summer and decrease in autumn is seen in the TC rain ratio, but its signal is not

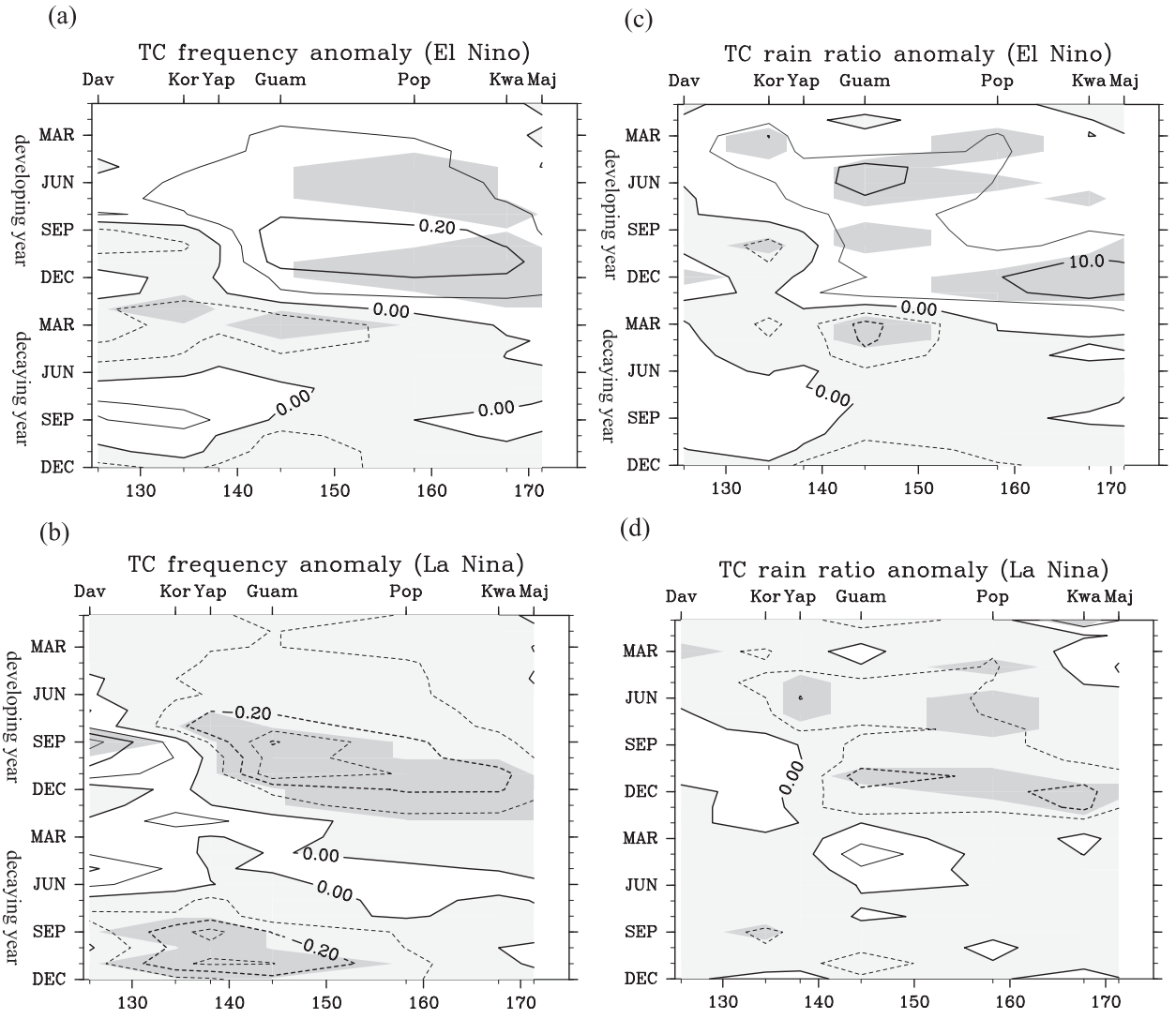


FIG. 5. Evolution of the anomalous (a),(b) three-month running-mean TC frequency and (c),(d) TC rain ratio from the developing to the decaying year of El Niño and La Niña, respectively, along the east–west island chain. Negative values are lightly shaded. Contour intervals are 0.1 TC month$^{-1}$ in (a),(b) and 5% in (c),(d). The heavily shaded area is the statistical significance at the 95% confidence level.

above the significant level. On the other hand, during the La Niña developing year, the opposite contrast of TC frequency appears south of 24°N. A significantly negative anomaly of TC rain ratio appears in April and May in Aparri and Catbalogan. Then, the anomaly turns to positive in September and October in the Philippines and during November in Taiwan. A strongly negative anomaly of the TC rain ratio appeared in November and December during La Niña decaying years.

### b. *Relationship between ENSO and different types of rainfall*

As shown in the previous subsection, the rainfall associated with TCs increases significantly along the east–west island chain during El Niño developing years. However, the total rainfall decreases from autumn to the following spring in the WNP during El Niño (Ropelewski and Halpert 1987). To clarify the relationship between ENSO and different types of rainfall (TC rainfall and non-TC rainfall), we calculate the regressions of each type of rainfall anomaly with reference to Niño-3.4 SST (an ENSO index that is the average SST anomaly over the region from 5°N to 5°S, from 170° to 120°W). First, we calculate the regression between the three-month-average (seasonal) rainfall anomaly and the mature phase of Niño-3.4 SST in December–February (DJF). We obtain how much rainfall change is associated with the SST change. Then, this regressed rainfall is divided by the corresponding seasonal-mean rainfall to obtain a percentage deviation from the seasonal mean. Each type of

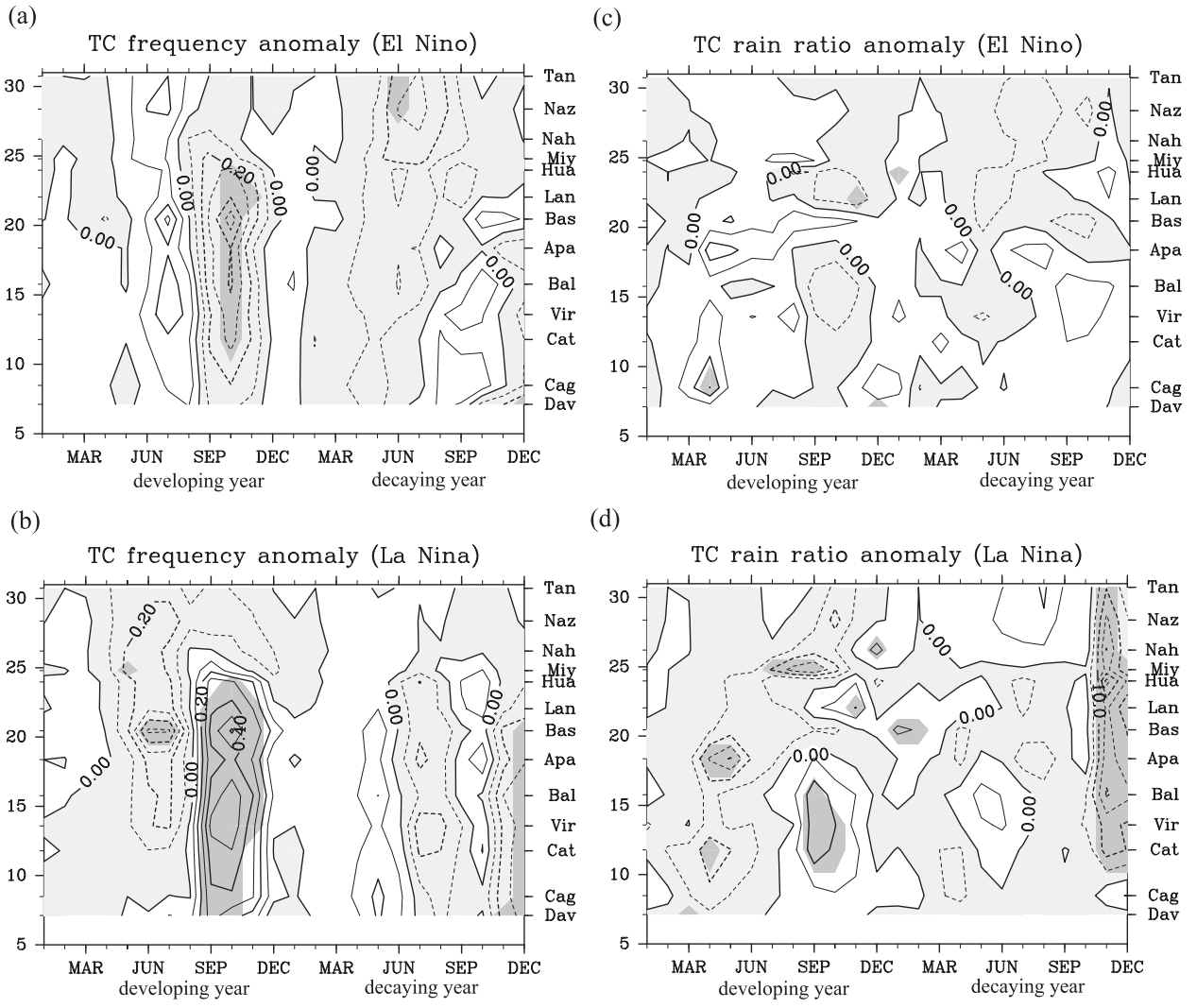


FIG. 6. As in Fig. 5, but for the north–south island chain.

rainfall (TC rainfall and non-TC rainfall) is regressed the same way.

Figure 7a shows the percentage seasonal-mean rainfall anomalies in JJA of El Niño/La Niña developing years. The total rainfall increases (decreases) significantly at several stations in the Philippines and the western Pacific islands along 10°N in JJA of El Niño (La Niña) developing years. The TC rainfall increases significantly over the western Pacific islands and increases more than 100% at the easternmost islands of Kwajalein and Majuro. Since non-TC rainfall does not have any significant changes over the western Pacific islands, the seasonal rainfall anomalies are mainly induced by anomalous TC activity.

In autumn (from September to November) of El Niño (La Niña) developing years, the total rainfall decreases (increases) significantly in Taiwan, the Philippines, and the western part of Pacific islands of Koror and Yap (Fig. 7b). However, in the Pacific islands east of Guam, the total rainfall does not have any significant changes because of the cancellation between increasing TC rainfall and decreasing non-TC rainfall.

In winter (from December to February) of the mature phase of El Niño (La Niña), regions of significant decrease (increase) in total rainfall spread widely over the WNP because of a decrease (increase) in non-TC rainfall (Fig. 7c). A significant increase of TC rainfall is seen only in Kwajalein and Majuro, but it cannot offset the decrease of non-TC rainfall. A significant increase of rainfall is seen on the southwest islands of Japan as a result of the increase of non-TC rainfall.

During spring of El Niño (La Niña) decaying years [from March to May, or MAM (1)], the total rainfall and non-TC rainfall show negative (positive) anomaly features

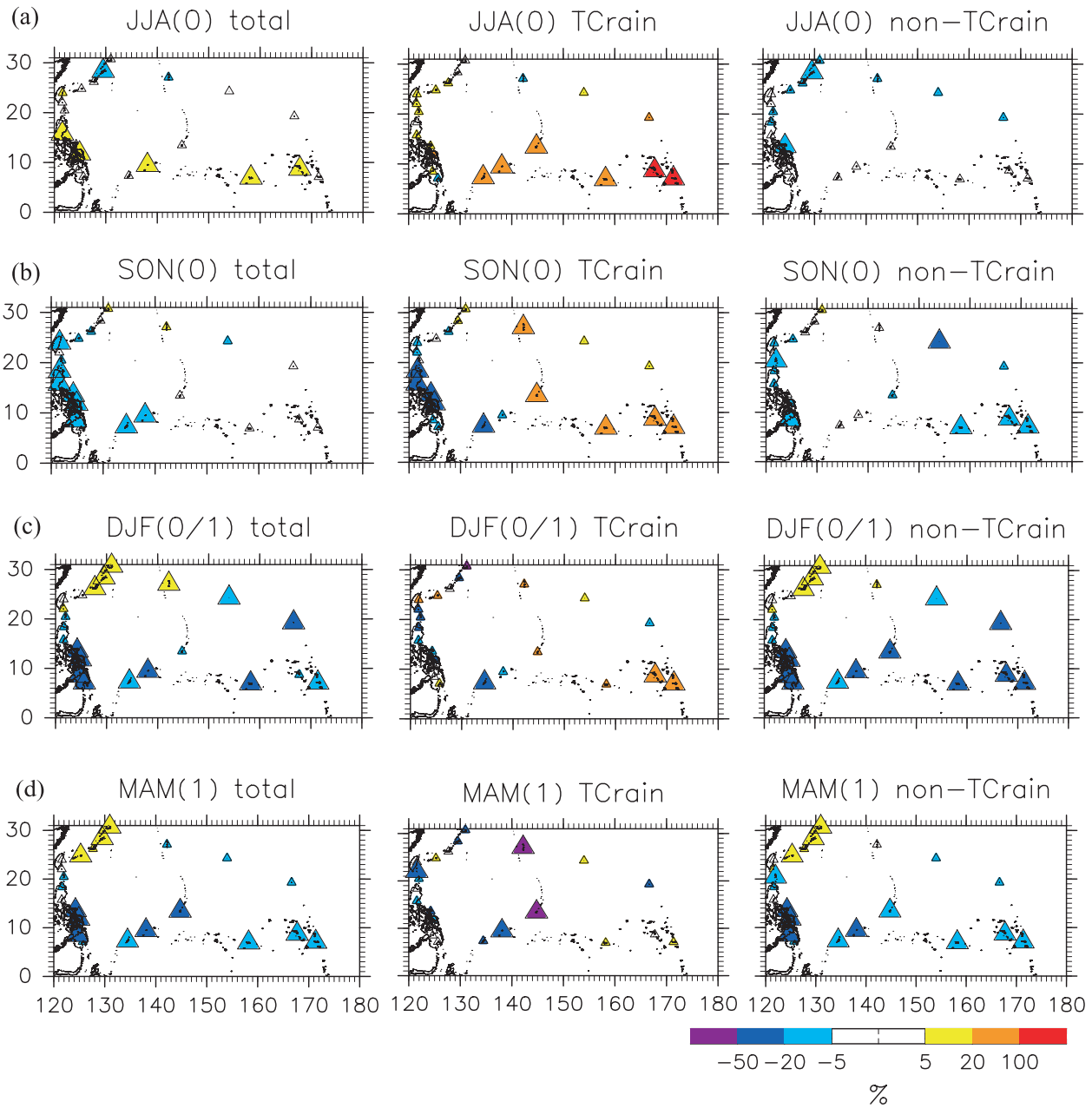


FIG. 7. (a) (left) Regressed total rainfall, (middle) TC rainfall, and (right) non-TC rainfall anomalies during summer of El Niño/La Niña developing year or JJA (0). The regression was made with respect to the Niño-3.4 SST in the mature phase of DJF (0/1), where 0 and 1 denote the El Niño/La Niña developing and decaying years, respectively. The regressed rainfall has been divided by the corresponding seasonal means. (b)–(d) Same as (a), but for SON (0), DJF (0/1), and MAM (1), respectively. Larger symbols represent that the correlation coefficient is statistically significant at the 95% confidence level. Color shadings indicate the regressions of rainfall anomalies.

similar to those in the previous winter (Fig. 7d). However, there is no significant increase in TC rainfall during MAM, instead a decrease in TC rainfall of more than 50% is seen in Guam and Chichijima. Similarly, increasing rainfall features are seen in the southwest islands of Japan.

### *c. Interannual variation of different types of rainfall*

The TC and non-TC rainfalls have different correlations with ENSO, as shown in the previous subsection. Which rainfall type is more dominant for the interannual variability seen in the total rainfall? Here, the

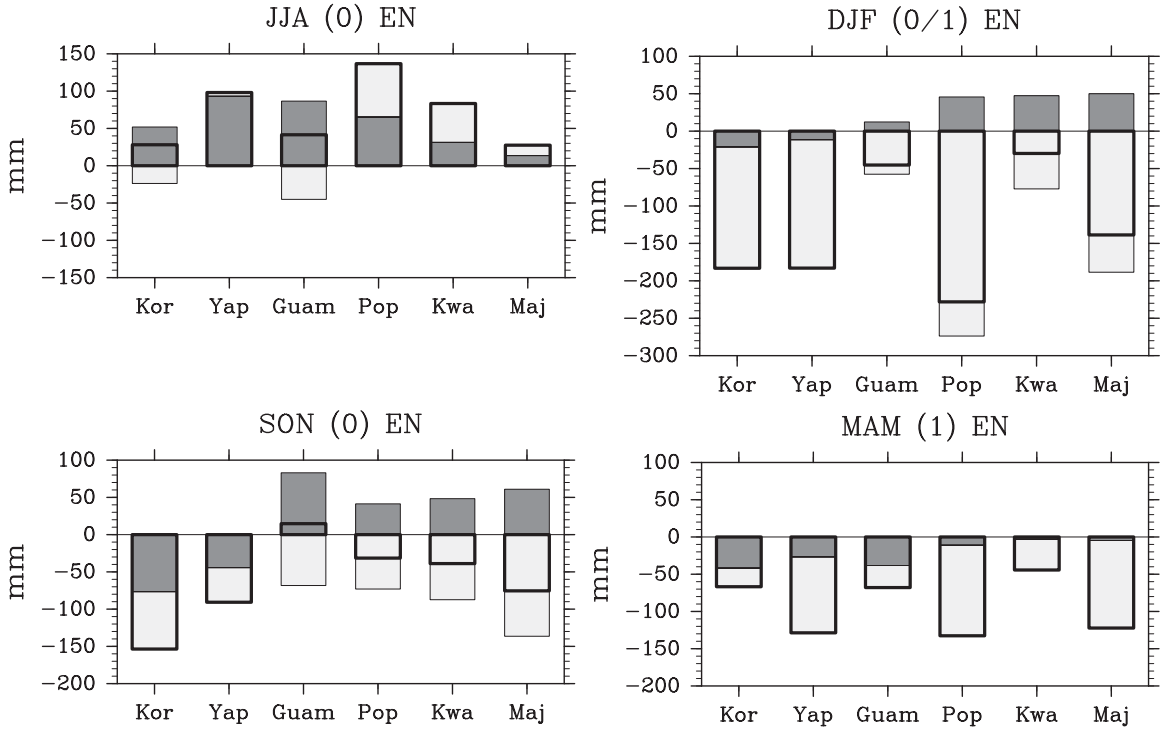


FIG. 8. Composite seasonal anomalies along the east–west island chain shown in Fig. 1 from JJA (0) of El Niño developing year to MAM (1) of El Niño decaying year. The bold, darkly shaded, and lightly shaded bars represent the total rainfall, TC rainfall, and non-TC rainfall, respectively.

contribution of each rainfall type to the total rainfall variability is evaluated quantitatively. Figure 8 shows the composite seasonal-mean (total, TC, and non-TC) rainfall anomalies during El Niño years along the 10°N cross section. In summer (JJA), the TC rainfall has positive anomalies at all stations. The increase of TC rainfall is a dominant factor for the increase of total rainfall from Koror to Guam. In SON, the non-TC rainfall has negative anomalies at all stations. On the other hand, the TC rainfall has positive anomalies to the east of Guam. The positive TC rainfall anomalies suppress the decrease in non-TC rainfall, resulting in normal or weak negative anomalies in total rainfall. In DJF, the TC rainfall still has positive anomalies to the east of Guam, but the magnitude is smaller than that of the negative non-TC rainfall anomalies. The contribution of the TC rainfall to the total rainfall anomalies becomes smaller compared to that in SON. In spring of El Niño decaying years [MAM (1)], the negative TC rainfall anomalies contribute significantly to the decrease in total rainfall in Koror and Guam. However, the non-TC rainfall anomalies play a dominant role in total rainfall at other stations.

Figure 9 shows seasonal-mean (total, TC, and non-TC) rainfall anomalies along the 125°E cross section during El Niño and La Niña. TC rainfall anomalies have a dominant effect on the decrease (increase) of total rainfall in autumn of El Niño (La Niña) years from Catbalogan of the Philippines to Huialien of Taiwan (except for Basco). The dominant effect of TC rainfall starts from August in Hualien, from September in Aparri and Lanyu, and from October at other southern stations (not shown). In winter (DJF) of El Niño (La Niña) years, negative (positive) non-TC rainfall anomalies become a dominant factor for the decrease (increase) in total rainfall south of Basco. However, the magnitudes are not symmetric with respect to El Niño and La Niña years. The northeasterly monsoon is activated during La Niña winter and produces a lot of non-TC rainfall along the east coast of the Philippines (Chen and Houze 1997; Zhang et al. 1997). In the summer of El Niño (La Niña) developing years, the increase (decrease) of total rainfall and TC rainfall appear in Baler and Catbalogan (Lyon et al. 2006; Lyon and Camargo 2008). However, these features are not general to other stations in the Philippines. Asymmetric TC rainfall anomalies appear in the southwest islands of Japan (Okinawa) and Taiwan. During El Niño years, TC rainfall shows negative anomalies in summer of decaying years in both Okinawa and Taiwan. During La Niña years, TC rainfall indicates positive anomalies in Okinawa but negative anomalies in Taiwan and Miyakojima in summer of both developing and decaying years.

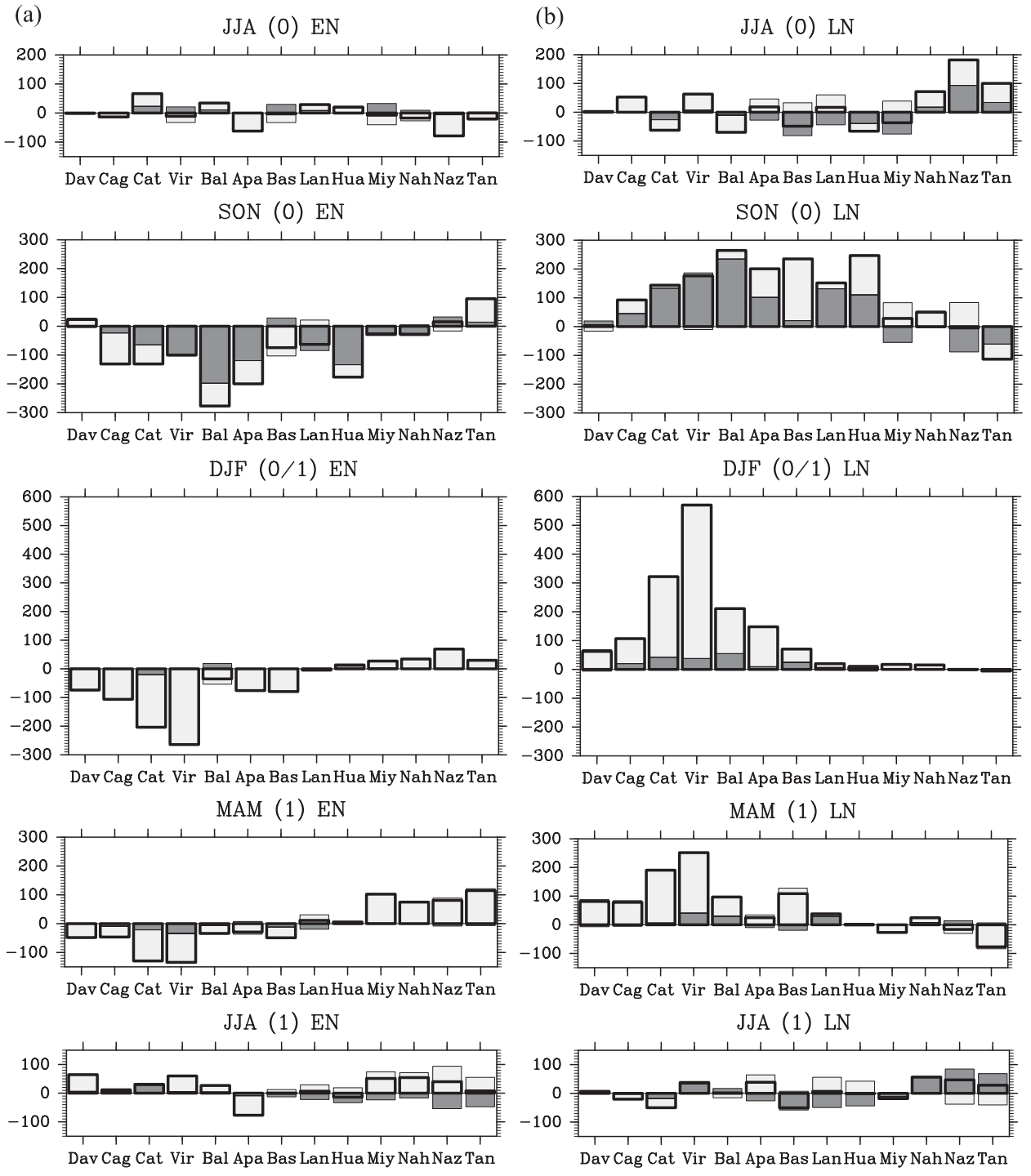


FIG. 9. (a) As in Fig. 8, but along the meridional island chain shown in Fig. 1. (b) As in (a), but for La Niña events.

### *d. Effect of TC formation and tracks on the TC rainfall*

In autumn of El Niño developing years, the warmest SST region shifts eastward to the equatorial central Pacific region and so does the large-scale upward-motion region associated with the Walker circulation (Rasmusson and Carpenter 1982; Philander 1990). This large-scale environment becomes unfavorable for developing convection over the WNP, which decreases

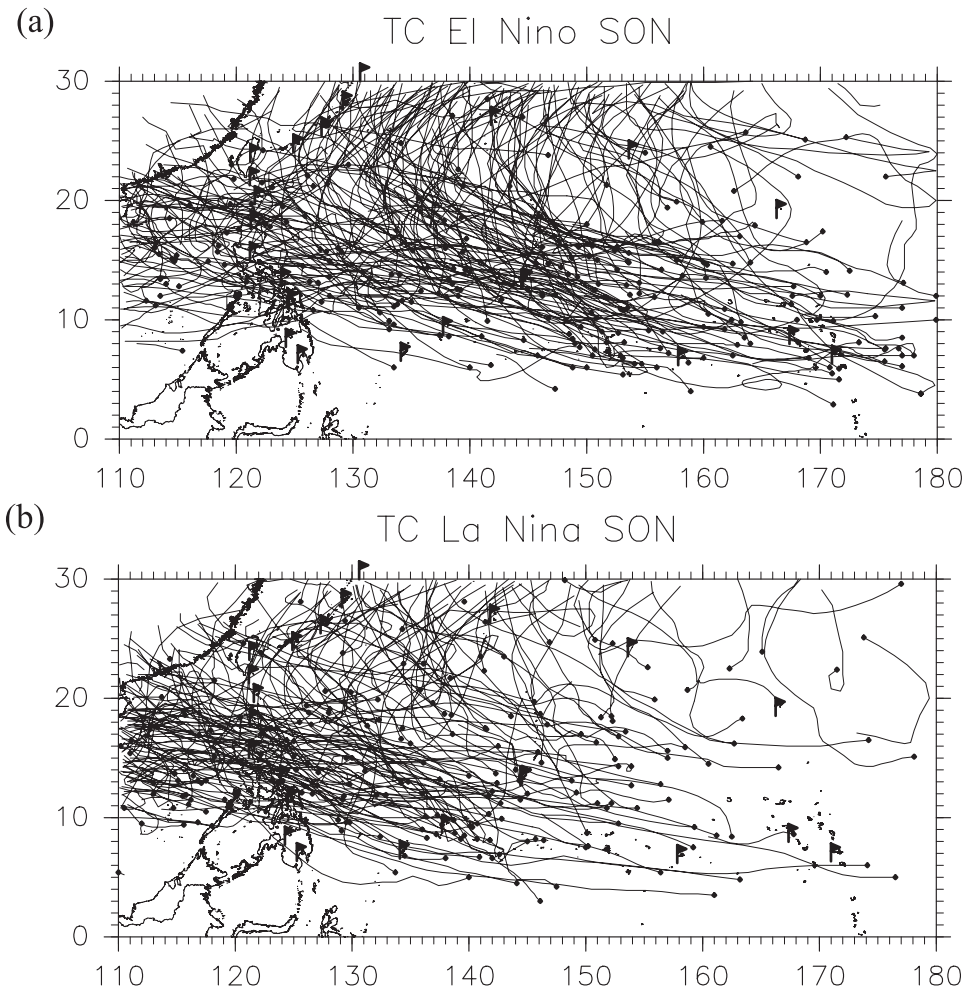


FIG. 10. TC genesis locations and tracks during SON of (a) El Niño and (b) La Niña developing years. Stations used in this study are indicated by flags.

non-TC rainfall at all stations along 10°N (Fig. 8). However, the TC rainfall significantly increases to the east of Guam. The origins of non-TC and TC rainfalls differ at these stations.

Figure 10 shows the locations of TC genesis and the tracks from the stage of tropical depression during SON of El Niño/La Niña developing years. The location of TC genesis shifts eastward during El Niño years, as mentioned earlier (cf. Wang and Chan 2002). This fact explains one of the reasons for an increase in TC rainfall in the eastern part of the island chain along 10°N. Another important issue is TC tracks. Despite the eastward shift of TS genesis locations, TCs move west-northwestward. They produce a lot of TC rainfall along their passages. The major path of TC tracks becomes important for producing rainfall at each station. Guam is under the influence of the major path of TC tracks in SON of El Niño years. On the other hand, Koror and Yap are not on the major path. This result can explain the significant increase of TC rainfall in and to the east of Guam and the decrease in Koror and Yap.

## 5. Conclusions

The effects of TCs on seasonal and interannual variability of the total rainfall over the WNP are investigated using rainfall data from 22 stations. The TC rainfall at each station is estimated by using an empirical function of the distance between the TC center and the station. On average, rainfall decreases with an increasing distance from the TC center. More than 1000 km away from the TC center, rainfall becomes nearly independent of the distance. TC rainfall is obtained by the accumulating rainfall when a TC is located within a 1000-km radius of the station. The spatial–temporal variability of the proportion of the TC rainfall is

examined along an east–west island chain near 10°N (between 7° and 13°N) and also a north–south chain near 125°E (between 120° and 130°E).

Along 10°N, the seasonality of total rainfall is mainly determined by non-TC rainfall that is influenced by the WNP monsoon trough. The proportion of the TC rain is relatively low. During the TC season from July to December, the TC rain ratio reaches on average 30% in Guam, decreases to 15%–23% in Koror and Yap, and to less than 10% at other stations. In contrast, along 125°E and between 18° and 26°N, the TC rain accounts for 50%–60% of the total rainfall during the TC season from July to October. The non-TC rainfall decreases after July under the influence of the WNP subtropical high. TC rainfall has a great effect from July to October along the north–south cross section of 125°E. The important factors for increasing the seasonal TC rain ratio are the higher frequency of TCs approaching the station and the closer passage of TCs from the station.

The interannual variability of TC formation is strongly affected by the phase of ENSO. In El Niño developing and mature phases from March to the following January, the TC rain ratio becomes higher than its climatology along 10°N. The region of significantly high TC rain ratio extends eastward from Guam in May to Majuro in October. In La Niña developing years, the significantly negative anomaly of TC rain ratio appears in April and May in Aparri and Catbalogan. Then, the anomaly turns positive during September and October in the Philippines and during November in Taiwan.

During summer of El Niño developing years, the increase of TC rainfall is significantly correlated with the mature phase of Niño-3.4 SST over the western Pacific islands. However, non-TC rainfall does not show any significant change. This suggests that a developing El Niño affects summer rainfall through increasing TC activity in the WNP. In the following autumn, the TC rainfall and total rainfall decrease significantly in Taiwan, the Philippines, and the western part of Pacific islands of Koror and Yap. However, in the Pacific islands east of Guam, the total rainfall does not have any significant change because of the cancellation between increasing TC rainfall and decreasing non-TC rainfall. In winter of the El Niño mature phase, a region with significantly decreasing total rainfall spreads widely over the WNP as a result of the decrease in non-TC rainfall.

In summer of El Niño developing years, the TC rainfall is a dominant factor for the increasing total rainfall from Koror to Guam. In autumn, the non-TC rainfall shows negative anomalies at all stations; however, the TC rainfall exhibits positive anomalies at and to the east of Guam. These positive TC rainfall anomalies cancel the negative anomalies of non-TC rainfall. In winter (DJF), the TC rainfall still has a positive anomaly at and to the east of Guam; However, the magnitude is smaller than that of negative non-TC rainfall anomalies. The contribution of TC rainfall to the total rainfall anomalies becomes smaller.

During autumn of El Niño (La Niña) years, TC rainfall has a dominant effect on the decreasing (increasing) total rainfall along 125°E from Catbalogan to Hualien. In winter of El Niño (La Niña) mature phase, negative (positive) non-TC rainfall anomalies become a dominant factor for decreasing (increasing) total rainfall in the Philippines. However, their magnitudes are not symmetric with respect to El Niño and La Niña. Asymmetric TC rainfall anomalies appear in Okinawa and Taiwan during summer of developing and decaying phases.

In autumn of El Niño developing years, the Walker circulation is shifted eastward and large-scale environment becomes unfavorable for developing convection over the WNP islands. Non-TC rainfall decreases over these islands. The locations of TC genesis also shift eastward in El Niño years. These TCs move westnorthwestward and produce abundant rainfall at and to the east of Guam along their passages. TC rainfall increases and offsets the negative anomalies of non-TC rainfall. Therefore, the total rainfall changes little in these regions. The results here suggest that in the tropical WNP and subtropical East Asian monsoon regions (east of 120°E), the seasonal and interannual variations of rainfall are controlled by changes in nonlocal circulations. These changes outside the monsoon domain may substantially affect summer monsoon rainfall by changing the TC's genesis and tracks.

*Acknowledgments.* We thank Drs. Jun Matsumoto and Ikumi Akasaka of Tokyo Metropolitan University for providing rainfall data in the Philippines. We also thank Ms. Yun-Lan Chen at the Central Weather Bureau of Taiwan for providing rainfall data in Taiwan. GFD-DENNOU library was used for drawing the figures.

## APPENDIX

### Limitations of the TC-Induced Rainfall Calculation

There are several limitations in calculating TC-induced rainfall using the station data. One limitation is the definition of TC rainfall that we use. In this study, the TC-induced rainfall is obtained by assuming that the TC affects a station rainfall when it falls in a radial distance of less than 1000 km from the station. JTWC defines the size of TC by the distance from the center to the

outermost enclosed isobar and reports the size of the TC as medium if the radius is from 3° to 6°, large if it is from 6° to 8°, and very large if it is more than 8°. In comparison, our definition of TC-induced rainfall domain of 1000 km is large. In reality, individual TCs vary in size and intensity. When the horizontal scale of a TC's outer rainband is smaller than the threshold we set, we may include the outer downdraft-suppressed region and/or rainfall not related to the TC circulation. These ambiguous factors can affect the accuracy in our calculation of the TC rainfall. However, the features we report are still robust and independent to the radius we choose to define TC rainfall (figure not shown).

Another limitation is the area that the 22 rain gauge stations cover. In this study, we only analyze two cross sections (an east–west island chain along 10°N and a north–south chain along 125°E). The location of TC genesis concentrates along 10°N from January to June and from October to December (Cheung 2004). Except for those months, the majority of TC genesis and the path are located north of 10°N. Therefore the east–west chain stations receive only part of the TC rainfall. The effect of TCs also differs between the east and west coasts of the north–south chain stations. In this study, we focus on TCs that move primarily westward and/or northward over the WNP. Therefore, only east coast/side or small islands stations are chosen in the Philippines and Taiwan. Chen et al. (2007) analyzed the frequency of heavy rainfall in Taiwan and separated typhoon rainfall from nontyphoon rainfall. They showed that heavy typhoon rainfall prevailed on the east side of Taiwan because of a higher frequency of westward–northwestward movement of a typhoon from the Pacific. The seasonality of total rainfall is quite different between the east and west coast of the Philippines and Taiwan (Commonwealth of the Philippines 1939; Chen and Chen 2003; Akasaka et al. 2007). Southwesterly (northeasterly) wind associated with summer (winter) monsoons strongly influences orographic rainfall and produces more rainfall on the west (east) coast during summer (winter). Seasonal and interannual variability of TC rainfall on the west side of the Philippines (Zamboanga, Iloilo, Manila, and Vigan) and Taiwan (Kaohsuing and Taipei) are analyzed to confirm the east–west difference. The TC rain ratio is lower on the west side than on the east side in July and higher in November. These results support the enhancement (suppression) of southwesterly (northeasterly) monsoon rainfall on the west side during summer (winter). For interannual variability, the TC rain ratio increases mainly in Manila from the summer of La Niña developing years to the following spring. However, the dominant features of seasonal and interannual variability of the TC rainfall on the east and west sides of the islands are related (not shown).

## REFERENCES


Akasaka, I., W. Morishima, and T. Mikami, 2007: Seasonal march and its spatial difference of rainfall in the Philippines. *Int. J. Climatol.,* **27,** 715–725.

Atkinson, G. D., 1977: Proposed system for near real time monitoring of global tropical circulation and weather patterns. Preprints, *11th Tech. Conf. on Hurricanes and Tropical Meteorology,* Miami Beach, FL, Amer. Meteor. Soc., 645–652.

Camargo, S. J., and A. H. Sobel, 2005: Western North Pacific tropical cyclone intensity and ENSO. *J. Climate,* **18,** 2996–3006.

Chan, J. C. L., 1985: Tropical cyclone activity in the northwest Pacific in relation to the El Niño/Southern Oscillation phenomenon. *Mon. Wea. Rev.,* **113,** 599–606.

——, 2000: Tropical cyclone activity over the western North Pacific associated with El Niño and La Niña events. *J. Climate,* **13,** 2960–2972.

Chen, C.-S., and Y.-L. Chen, 2003: The rainfall characteristics of Taiwan. *Mon. Wea. Rev.,* **131,** 1323–1341.

——, ——, C.-L. Liu, P.-L. Lin, and W.-C. Chen, 2007: Statistics of heavy rainfall occurrences in Taiwan. *Wea. Forecasting,* **22,** 981–1002.

Chen, S. S., and R. A. Houze Jr., 1997: Interannual variability of deep convection over the tropical warm pool. *J. Geophys. Res.,* **102,** 25 783–25 795.

Chen, T.-C., S.-P. Weng, N. Yamazaki, and S. Kiehne, 1998: Interannual variation in the tropical cyclone formation over the western North Pacific. *Mon. Wea. Rev.,* **126,** 1080–1090.

Cheung, K. K. W., 2004: Large-scale environmental parameters associated with tropical cyclone formations in the western North Pacific. *J. Climate,* **17,** 466–484.

Commonwealth of the Philippines, 1939: *Climate of the Philippines*. Department of Agriculture and Commerce Bureau of Printing, 31 pp.

Dong, K., 1988: El Niño and tropical cyclone frequency in the Australian region and the northwest Pacific. *Aust. Meteor. Mag.,* **36,** 219–225.

Frank, W. M., 1977: The structure and energetics of the tropical cyclone I. Storm structure. *Mon. Wea. Rev.,* **105,** 1119–1135.

Fudeyasu, H., S. Iizuka, and T. Matsuura, 2006: Impact of ENSO on landfall characteristics of tropical cyclones over the western North Pacific during the summer monsoon season. *Geophys. Res. Lett.,* **33,** L21815, doi:10.1029/2006GL027449.

Lander, M. A., 1993: Comments on ''A GCM simulation of the relationship between tropical storm formation and ENSO.'' *Mon. Wea. Rev.,* **121,** 2137–2143.

——, 1994: An exploratory analysis of the relationship between tropical storm formation in the western North Pacific and ENSO. *Mon. Wea. Rev.,* **122,** 636–651.

Lau, K.-M., G. J. Yang, and S. H. Shen, 1988: Seasonal and intraseasonal climatology of summer monsoon rainfall over East Asia. *Mon. Wea. Rev.,* **116,** 18–37.

Lyon, B., and S. J. Camargo, 2008: The seasonally-varying influence of ENSO on rainfall and tropical cyclone activity in the Philippines. *Climate Dyn.,* **32,** 125–141.

——, H. Cristi, E. R. Verceles, F. D. Hilario, and R. Abastillas, 2006: Seasonal reversal of the ENSO rainfall signal in the Philippines. *Geophys. Res. Lett.,* **33,** L24710, doi:10.1029/2006GL028182.

Matsumoto, J., 1992: The seasonal changes in Asian and Australian monsoon regions. *J. Meteor. Soc. Japan,* **70,** 257–273.

Ninomiya, K., and T. Akiyama, 1992: Multi-scale features of Baiu, the summer monsoon over Japan and the East Asia. *J. Meteor. Soc. Japan,* **70,** 467–495.

Philander, S. G. H., 1990: *El Niño, La Niña and the Southern Oscillation*. Academic Press, 289 pp.

Rao, G. V., and P. D. MacArthur, 1994: The SSM/I estimated rainfall amounts of tropical cyclones and their potential in predicting the cyclone intensity changes. *Mon. Wea. Rev.,* **122,** 1568–1574.

Rasmusson, E. M., and T. H. Carpenter, 1982: Variations in tropical sea surface temperature and surface wind fields associated with the Southern Oscillation/El Niño. *Mon. Wea. Rev.,* **110,** 354–384.

Rayner, N. A., D. E. Parker, E. B. Horton, C. K. Folland, L. V. Alexander, D. P. Rowell, E. C. Kent, and A. Kaplan, 2003: Global analyses of sea surface temperature, sea ice, and night marine air temperature since the late nineteenth century. *J. Geophys. Res.,* **108,** 4407, doi:10.1029/2002JD002670.

Rodgers, E. B., and R. F. Adler, 1981: Tropical cyclone rainfall characteristics as determined from a satellite passive microwave radiometer. *Mon. Wea. Rev.,* **109,** 506–521.

——, ——, and H. F. Pierce, 2000: Contribution of tropical cyclones to the North Pacific climatological rainfall as observed from satellites. *J. Appl. Meteor.,* **39,** 1658–1678.

Ropelewski, C. F., and M. S. Halpert, 1987: Global and regional scale precipitation patterns associated with the El Niño/Southern Oscillation. *Mon. Wea. Rev.,* **115,** 1606–1626.

Trenberth, K. E., 1997: The definition of El Niño. *Bull. Amer. Meteor. Soc.,* **78,** 2771–2777.

Wang, B., 1994: Climatic regimes of tropical convection and rainfall. *J. Climate,* **7,** 1109–1118.

——, and J. C. L. Chan, 2002: How strong ENSO events affect tropical storm activity over the western North Pacific. *J. Climate,* **15,** 1643–1658.

——, and Q. Zhang, 2002: Pacific–East Asia teleconnection. Part II: How the Philippine Sea anomalous anticyclone is established during El Niño development. *J. Climate,* **15,** 3252–3265.

——, R. Wu, and X. Fu, 2000: Pacific–East Asian teleconnection: How does ENSO affect East Asia climate? *J. Climate,* **13,** 1517–1536.

Wu, G., and N.-C. Lau, 1992: A GCM simulation of the relationship between tropical-storm formation and ENSO. *Mon. Wea. Rev.,* **120,** 958–977.

Wu, M. C., W. L. Chang, and W. M. Leung, 2004: Impacts of El Niño–Southern Oscillation events on tropical cyclone landfalling activity in the western North Pacific. *J. Climate,* **17,** 1419–1428.

Xie, P., and P. A. Arkin, 1996: Analysis of global monthly precipitation using gauge observations, satellite estimates, and numerical model predictions. *J. Climate,* **9,** 840–858.

Zhang, Y., K. R. Sperber, and J. S. Boyle, 1997: Climatology and interannual variation of the East Asian winter monsoon: Results from the 1979–95 NCEP/NCAR reanalysis. *Mon. Wea. Rev.,* **125,** 2605–2619.